Regional and tissue specific transcript signatures of ion channel genes in the non-diseased human heart

Nathalie Gaborit[1,2], Sabrina Le Bouter[3], Viktoria Szuts[4], Andras Varro[4,5], Denis Escande[1], Stanley Nattel[3] and Sophie Demolombe[1]

[1] *INSERM, U533, Nantes, F-4400 France*

[2] *Université de Nantes, faculté de Médecine, Nantes, F-4400 France*

[3] *Montreal Heart Institute and Université de Montréal, Montreal, Quebec, Canada*

[4] *Department of Pharmacology and Pharmacotherapy, University of Szeged, Szeged, Hungary*

[5] *Division for Cardiovascular Pharmacology, Hungarian Academy of Sciences, Szeged, Hungary*

The various cardiac regions have specific action potential properties appropriate to their electrical specialization, resulting from a specific pattern of ion-channel functional expression. The present study addressed regionally defined differential ion-channel expression in the non-diseased human heart with a genomic approach. High-throughput real-time RT-PCR was used to quantify the expression patterns of 79 ion-channel subunit transcripts and related genes in atria, ventricular epicardium and endocardium, and Purkinje fibres isolated from 15 non-diseased human donor hearts. Two-way non-directed hierarchical clustering separated atria, Purkinje fibre and ventricular compartments, but did not show specific patterns for epicardium *versus* endocardium, nor left- *versus* right-sided chambers. Genes that characterized the atria (*versus* ventricles) included Cx40, Kv1.5 and Kir3.1 as expected, but also Cav1.3, Cav3.1, Cav$\alpha2\delta2$, Nav$\beta1$, TWIK1, TASK1 and HCN4. Only Kir2.1, RyR2, phospholamban and Kv1.4 showed higher expression in the ventricles. The Purkinje fibre expression-portrait (*versus* ventricle) included stronger expression of Cx40, Kv4.3, Kir3.1, TWIK1, HCN4, ClC6 and CALM1, along with weaker expression of mRNA encoding Cx43, Kir2.1, KChIP2, the pumps/exchangers Na$^+$,K$^+$-ATPase, NCX1, SERCA2, and the Ca^{2+}-handling proteins RYR2 and CASQ2. Transcripts that were more strongly expressed in epicardium (*versus* endocardium) included Cav1.2, KChIP2, SERCA2, CALM3 and calcineurin-α. Nav1.5 and Nav$\beta1$ were more strongly expressed in the endocardium. For selected genes, RT-PCR data were confirmed at the protein level. This is the first report of the global portrait of regional ion-channel subunit-gene expression in the non-diseased human heart. Our data point to significant regionally determined ion-channel expression differences, with potentially important implications for understanding regional electrophysiology, arrhythmia mechanisms, and responses to ion-channel blocking drugs. Concordance with previous functional studies suggests that regional regulation of cardiac ion-current expression may be primarily transcriptional.

Cardiac function depends on the appropriate timing of contraction in each region, as well as on an appropriate beating rate. The various cardiac regions are characterized by specific action potential (AP) shapes, resulting from regionally defined complements of ionic currents (Schram *et al.* 2002). For example, it is well known that the density of the inward-rectifier K$^+$-current I_{K1} is larger

in ventricles than atria, whereas the density of the acetylcholine-activated K$^+$-current I_{KACh} is larger in atria (Schram *et al.* 2002). Accordingly, transcripts for the inwardly rectifying K$^+$-channel subunit Kir2.1 (mediating I_{K1}) are more strongly expressed in the ventricle (Dhamoon *et al.* 2004), whereas transcripts for Kir3.1 (encoding I$_{KACh}$ channels) are predominantly expressed in the atria (DePaoli *et al.* 1994). A higher density of the transient outward current, I_{to}, is characteristic of epicardium *versus* endocardium, in parallel with stronger

This paper has online supplemental material.

expression of KChIP2 transcripts in the epicardium (Rosati *et al.* 2001). In addition to its role in normal cardiac electrical functioning, electrical heterogeneity also contributes to a variety of cardiac arrhythmia mechanisms (Schram *et al.* 2002; Antzelevitch, 2004).

To date, however, studies of ion-transporter subunit distribution within specific regions of the human heart have been limited to a small number of candidate subunits believed to be of importance. Additionally, limited access to healthy human cardiac tissue samples has forced most investigators to work with explanted cardiac-transplant recipient hearts, generally strongly affected by heart disease. Recent progress in genomics, particularly for mouse and man, has led to the identification of a detailed repertoire of ion-channel genes. In parallel, recently developed high-throughput quantitative molecular biology techniques permit simultaneous measurement of the expression of up to hundreds of genes, thereby permitting the creation of a global portrait of ion-channel expression (Marionneau *et al.* 2005). In the present study, we used a high-throughput quantitative approach to assess regionally defined expression of genes encoding ion-channel and transporter subunits in the non-diseased human heart.

Methods

Human tissue samples

Non-diseased human hearts that were technically unusable for transplantation (based on logistical, not patient-related, considerations) were obtained from organ donors. Before cardiac explantation, organ donor patients did not receive medication except dobutamine, furosemide and plasma expanders. The investigations conform to the principles outlined in the *Declaration of Helsinki* of the World Medical Association. All experimental protocols were approved by the Ethical Review Board of the Medical Center of the University of Szeged (No. 51-57/1997 OEJ). Human cardiac tissue was dissected from 15 donors (44 ± 12 years; mean $\pm$ s.d.; min 18; max 65; 7 women and 8 men) and stored in cardioplegic solution at 4°C for 4–8 h before being frozen in liquid nitrogen.

Left and right atrial (LA and RA) samples were dissected from the tip of the appendages. Transmural left and right ventricular (LV and RV) tissue samples were consistently obtained from the basal region of the heart. Selective left and right epicardial (Lepi and Repi) and endocardial (Lendo and Rendo) tissues were obtained by cutting 1 mm thick slices from the epicardial and endocardial surfaces of the base, respectively (Zicha *et al.* 2004). Purkinje fibre mRNA was extracted from false tendons dissected from the ventricles.

Comparisons of gene expression between cardiac compartments were conducted within sets of samples from individual patients (except for Purkinje fibres), thus controlling for interindividual variability. Seven matching samples were available for LA *versus* LV comparison, five for RA *versus* RV, seven for Lepi *versus* Lendo, eight for Repi *versus* Rendo, five for LA *versus* RA, five for LV *versus* RV, six for Lepi *versus* Repi and six for Lendo *versus* Rendo. Purkinje fibres were obtained from eight donors.

The sampled hearts were macroscopically and microscopically normal. Lack of hypertrophy was further confirmed by measuring the expression of atrial natriuretic factor (ANF) transcripts (data not shown).

RNA preparation

Total RNA from each cardiac sample was isolated and DNase-treated with the RNeasy Fibrous Tissue Mini Kit (Qiagen) following manufacturer's instructions. The quality of total RNA was assessed with polyacrylamide-gel microelectrophoresis (Agilent 2100 Bioanalyser) and by reverse transcriptase-polymerase chain reaction (RT-PCR). Lack of genomic DNA contamination was verified by PCR.

TaqMan real-time reverse transcriptase-polymerase chain reaction

The TaqMan Low-Density Array (TLDA, Applied Biosystems) technology was used in a two-step RT-PCR process, as previously reported (Marionneau *et al.* 2005). Briefly, first-strand cDNA was synthesized from 2 μg of total RNA using the High-Capacity cDNA Archive Kit (Applied Biosystems). PCR reactions were then performed on TLDA with the ABI Prism 7900HT Sequence Detection System (Applied Biosystems). The 384 wells of each card were preloaded with 96×4 predesigned fluorogenic TaqMan probes and primers. Probes were labelled with the fluorescent reporter 6-carboxyfluorescein (FAM$^{\circledR}$, Applera Corp.) at the 5′-end and with non-fluorescent quencher on the 3′-end. The genes selected for their cardiac expression (listed in the online supplemental material) encode 72 ion channel α- and β-subunits, 17 Na$^+$,K$^+$-ATPase isoforms and proteins involved in calcium homeostasis, three hypertrophy markers (ANF, BNP, β-MHC) and four reference genes for normalization. Data were collected with instrument spectral compensation with Applied Biosystems SDS 2.1 software and analysed with the threshold cycle (C_t) relative-quantification method (Livak & Schmittgen, 2001). Ten genes (Cavγ4, Cavγ5, Cavγ6, CFTR, Kv1.1, Kv2.2, Kv3.1, Kv3.2, Kir1.1 and Nav1.4) were eliminated because their expression level frequently fell under the threshold for detection ($> 50\%$ undetermined data). Among the remaining genes, nine exhibited a maximum of 7% undetermined data and the remaining 70 exhibited no undetermined data point. We

selected the hypoxanthine guanine phosphoribosyl trans-ferase (*HPRT*) gene for data normalization, as the most uniformly distributed gene. The relative expression of each gene *versus* HPRT was calculated for each sample (ΔC_t indicates normalized data).

Data analysis

Data were analysed in three independent ways. (i) Two-way hierarchical agglomerative clustering was applied to the gene-expression matrix consisting of grouped biopsies and the 79 genes with valid expression involved in electrical signalling. We applied average linkage clustering with Pearson correlation using the Cluster software (Eisen *et al.* 1998). Clusters were visualized using the Treeview software. (ii) For each compartment, the relative expression of each gene *versus* HPRT ($2^{-\Delta C_t}$) was calculated and then averaged (data listed in the online supplemental material). (iii) For each gene and patient, the ratios between matching samples (atrium *versus* ventricle, epicardium *versus* endocardium, and left *versus* right compartments) were calculated and then averaged. For unmatched samples (Purkinje fibres *versus* RV) the ratio for each gene *versus* the mean RV was calculated and then averaged. Pair-wise comparisons between cardiac compartments were conducted on within-patient matched samples by Student's paired *t* test ($P < 0.05$ considered significant, $n = 5$–8). Unpaired *t* tests were used for unmatched samples.

Western blot

Proteins were extracted from four additional donor tissue samples, as previously described (Zicha *et al.* 2004). Proteins were fractionated on either 7.5% (Kv1.5, Kv4.3 and Cav1.3) or 10% (Cx40, KChIP2, and TWIK1) SDS-polyacrylamide gels and were transferred electro-phoretically to Immobilon-P polyvinylidene fluoride membranes (Millipore). Membranes were blocked and incubated with antibodies as previously described (Zicha *et al.* 2004). Kv1.5 polyclonal antibody (1 : 500 dilution) was purchased from Upstate; Cx40 (1 : 1000) and Kv4.3 (1 : 500) polyclonal antibodies were purchased from Chemicon Laboratories; Cav1.3 polyclonal antibody (1: 2000) was a kind gift from Dr Hiroshi Hibino (Osaka, Japan); TWIK1 polyclonal antibody (1 : 3000) was a kind gift from Dr Jacques Barhanin (Valbonne, France); and KChIP2 monoclonal antibody (1 : 1000) was a kind gift from Dr James Trimmer (Davis, USA). Protein loading was controlled by probing with anti-GAPDH anti-body (Research Diagnostics). After washing, membranes were incubated with horseradish peroxidase-conjugated anti-mouse or anti-rabbit IgG secondary antibody (1 : 10000, Santa Cruz). Bound antibodies were detected

with Western Lightening Chemiluminescence Reagent Plus (Perkin-Elmer Life Sciences). For each antibody, time exposure was similar for membranes containing atrial and ventricle samples and for membranes containing epicardial and endocardial samples. Band densities were measured using Scion Image (Scion Corp.).

Results

The transcriptional expression levels of 72 α- and β-ion channel subunits and 17 Na^+,K^+-ATPase isoforms and proteins involved in calcium homeostasis were investigated by high-throughput real-time RT-PCR. For 10 genes, expression was undetectable after 40 cycles of PCR amplification in any cardiac compartment. These were excluded from further analysis. All fluorescent probes had 100% PCR efficiency (Applied Biosystems application note). This standardized method permits quantitative comparison of expression levels among cardiac compartments and among genes.

Hierarchical clustering of Purkinje fibre, atrial and ventricular tissues

Two-way hierarchical clustering analysis groups samples according to gene-expression differences, with the most similar expression patterns located closest to each other and the most different patterns furthest apart. For visual appreciation, the samples are linked to a tree. The size of tree branches indicates the distance between clusters: larger branch sizes indicate greater separation among clusters. Hierarchical clustering analysis was applied to 32 atrial, ventricular and Purkinje fibre samples (Fig. 1). There was a first-order branch separation between atrial samples on one branch and ventricular and Purkinje fibre samples on the other, demonstrating full discrimination of atrial from ventricular compartments. In a second-order branch, Purkinje fibres clustered separately from ventricular myocardium. There was no overlap between primary compartments. That is, atrial, ventricular and Purkinje fibre samples clustered separately, indicating clearly different gene expression. The genes that were most relevant for clustering are indicated in Fig. 1. Group A contains genes that are more strongly expressed in Purkinje fibres *versus* working atrial or ventricular myocardium. These include Kv4.3, Kvβ3, MiRP1, KChAP, TASK2, ClC6, CALM1 and InsP3R1. Group B contains genes that are more abundant in atria and Purkinje fibres than in working ventricles, including, as expected for atria, Cx40, Kv1.5 and Kir3.1 (Schram *et al.* 2002), but also Cav1.3, Cav3.1, Cavα2δ2, Navβ1, MIRP3, TWIK1 and TASK1. No gene clusters with stronger ventricular-myocardial expression *versus* atrium were observed: i.e. atrial samples were distinct through over- rather than under-expression of
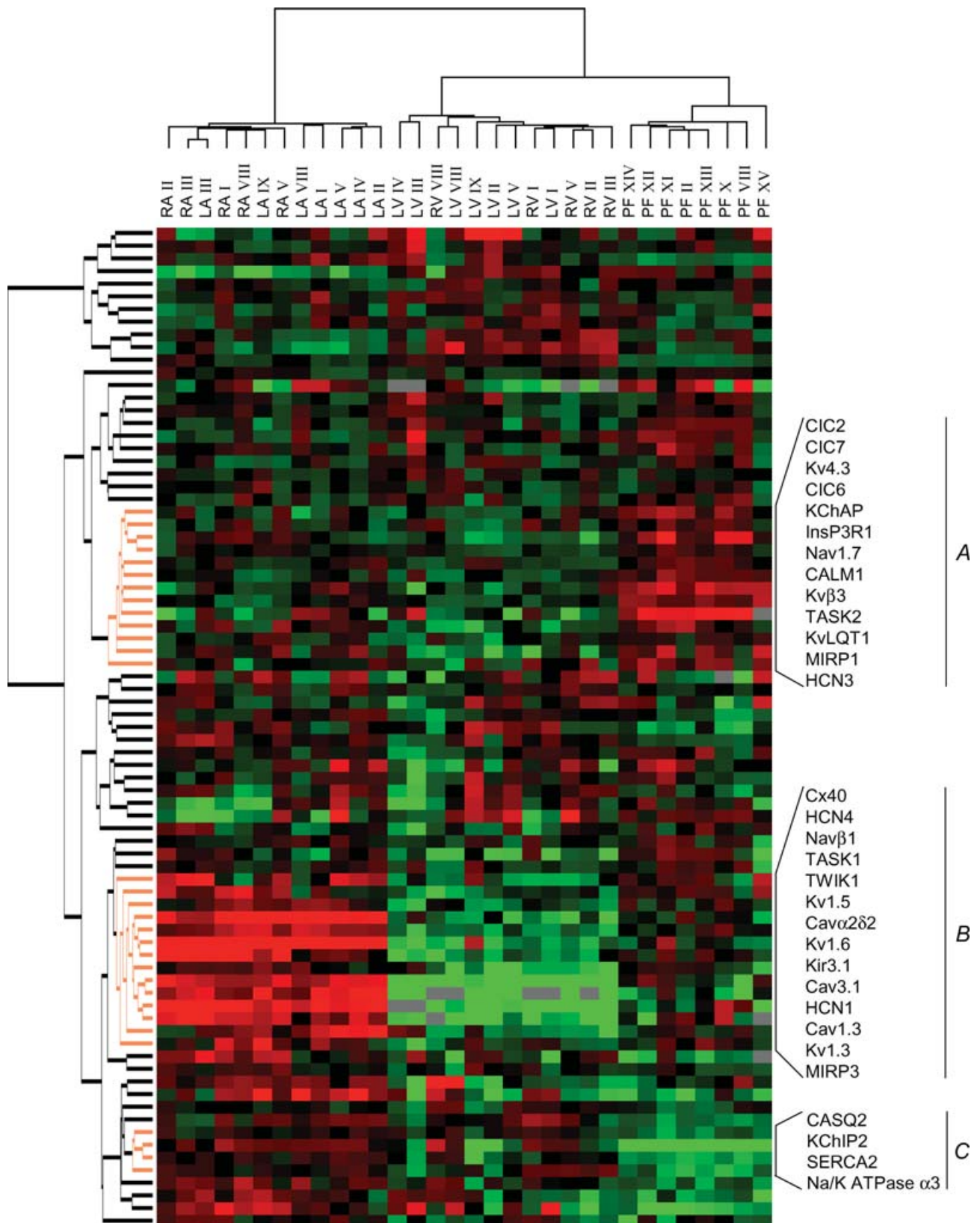
ion-channel subunit genes. Group C contains genes with relatively weaker expression in Purkinje fibres compared to atria or working ventricular tissues, including KChIP2, SERCA2 and CASQ2. Within atrial and ventricular clusters, samples from the left- *versus* right-sided cavities did not separate.

The same approach was applied to basal epicardial and endocardial samples. As shown in Fig. 2, epicardial and endocardial samples intermingled, with no distinct separation. Differences in ion-channel gene expression were thus not strong enough to discriminate epi- from the endocardial expression patterns. Since age and sex could affect cardiac electrophysiology by altering ion-channel gene expression, we performed hierarchical analysis with age and sex as covariates and saw no significant effects (data not shown). As for the tissue analysis shown in Fig. 1, there was no significant clustering of left *versus* right-sided transmural layer samples. The lack of left–right clustering in both Figs 1 and 2 indicates a lack of specific ion-channel gene signature for left- *versus* right-sided tissues.

Regional expression levels of ion-channel and transporter subunits

The method we used to quantify transcripts permits comparison of relative expression levels among genes (Tables 1–4). Among the Ca^{2+}-channel genes, the L-type Ca^{2+}-channel α-subunit Cav1.2 (α_{1c}) was the most strongly expressed overall, whereas the other L-type α-subunit (Cav1.3) showed much lower expression (Table 1A). The T-type Ca^{2+}-channel subunit Cav3.1 (α_{1G}) was expressed predominantly in the atrium and Cav3.2 (α_{1H}) showed lower-level expression. No significant expression of Cav3.3 (α_{1I}) was detected. The expression of Ca^{2+}-channel regulatory subunit transcripts (Cav$\alpha 2\delta 1$, Cav$\alpha 2\delta 2$, Cav$\beta 2$) was also strong.

As expected, Cx43 was the predominant connexin subunit in the ventricle (Table 1B). Cx40 predominated in the atria, with significant expression in Purkinje fibres that was about equal that of Cx43. Cx45 transcripts were detectable in all tissues. Among the voltage-gated sodium channel α-subunits, Nav1.5 (*SCN5A*) exhibited the highest expression (Table 1C). Nav2.1 (*SCN6A–SCN7A*) transcripts were also abundant. Nav$\beta 1$ was by far the most abundant β-subunit.

Within the Kv-channel α-subunit family, Kv1.5, Herg, Kv4.3 and KvLQT1 transcripts predominated (Table 2A). Kv1.5 transcripts were ~45-fold more strongly expressed in atrial *versus* ventricular tissues. Among K^+-channel β-subunits, KChIP2, MIRP3, SUR2, KChAP, MinK and MIRP2 were the most abundant mRNA species (Table 2B). KChIP2 exhibited the strongest intertissue variations, with very low-level expression in Purkinje fibres. SUR2 transcripts were much more abundant than SUR1.

Transcripts underlying the inwardly rectifying potassium current I_{K1} (Kir2.1, Kir2.2 and Kir2.3) were expressed in every cardiac region, whereas Kir3.1 (responsible for the muscarinic-gated K^+-channel I_{KACh}) predominated in the atria (Table 3A). Purkinje fibre expression of Kir3.1 was substantially greater than in ventricular muscle, consistent with the differential effects of muscarinic stimulation on Purkinje *versus* ventricular repolarization (Malfatto *et al.* 1996). Both Kir6.2 and Kir6.1 subunits were detectable and most strongly expressed in ventricles. Among the tandem two-pore domain K^+-channels, TWIK1 was strongly expressed, particularly in atria, and TASK1 also showed atrial-selective expression.

HCN4, HCN2 and HCN1 transcripts corresponding to the hyperpolarization-activated cyclic nucleotide-gated current (I_f), were detected in all tissues, with predominant atrial expression (Table 3B). Concerning Cl^- channel transcripts (Table 3C), our data showed a rank order of expression ClC7 > ClC6 > ClC3 >> ClC2, without major tissue-based differences. As previously observed in the mouse (Marionneau *et al.* 2005), exchangers and intracellular Ca^{2+} handling proteins expressed at ~10-times higher levels than ion-channel subunits (Table 4). The expression of SERCA2, RyR2 and phospholamban predominated over the other Ca^{2+}-handling regulators.

Relative expression of atrium *versus* ventricle

We next undertook in-depth comparisons of atrial *versus* ventricular expression levels. Because there is some consistency to overall function and conditions for right- *versus* left-sided chambers, we compared LA gene expression to that in LV, and RA expression to RV. Detailed comparisons between LA *versus* LV, as well as for RA *versus*

Figure 1. Two way hierarchical agglomerative clustering applied to 79 genes (vertically) and to 5 left and right atria (LA and RA), 7 left and right ventricles (LV and RV) and 8 Purkinje fibre samples (horizontally)
The input consisted of the ratio for each patient and gene *versus* reference gene. Each gene is represented by a single row of coloured boxes and each patient by a single column. The entire gene clustering is shown on the left. Three selected gene clusters are shown on the right (A–C) containing relevant genes for Purkinje fibres and working myocardium discrimination (A, C), and for atrial–ventricular discrimination (B). Each colour patch in the map represents the gene expression level in one sample from one patient, with expression levels ranging from bright green (lowest) to bright red (highest). Missing values are coded as silver.
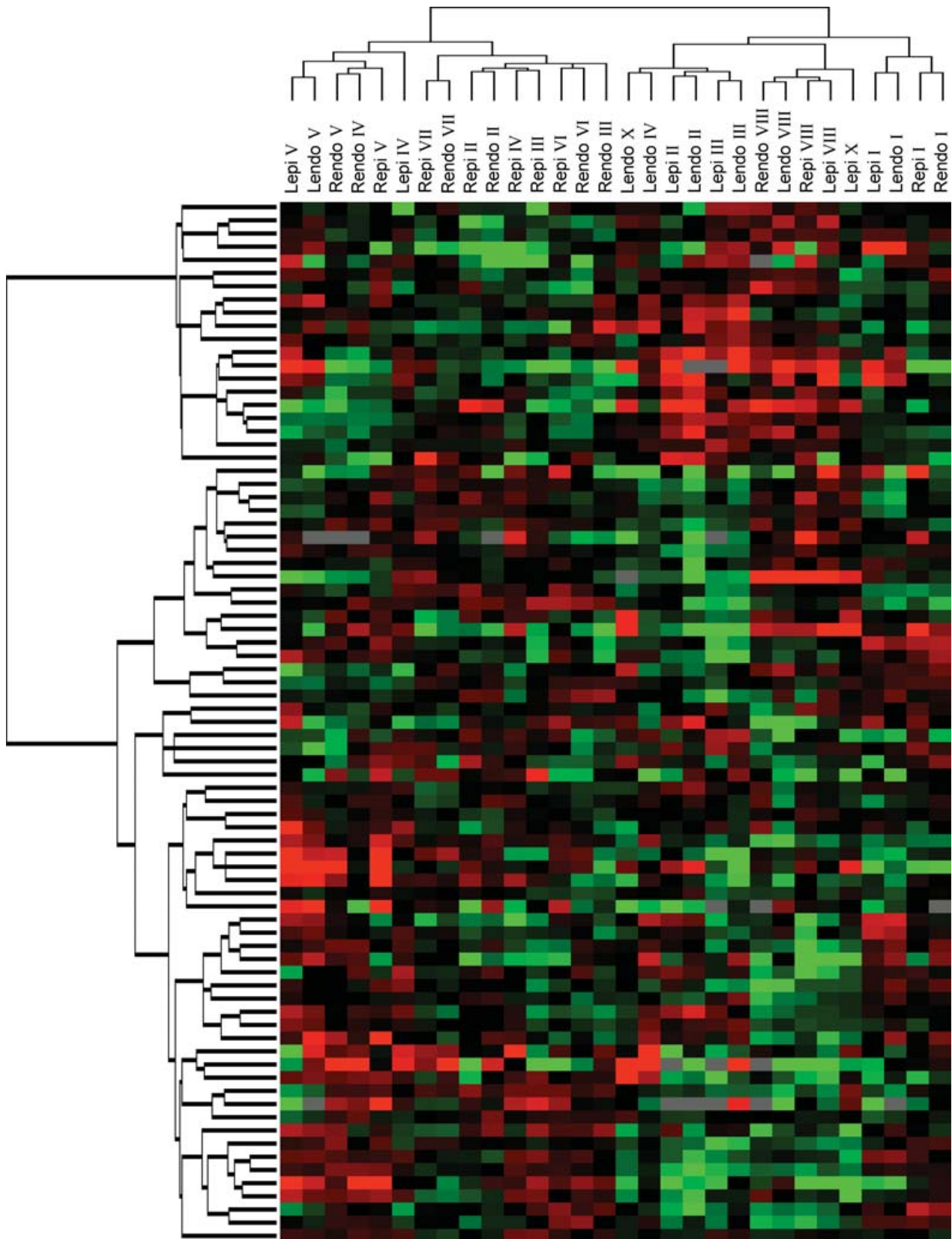
Figure 2. Two-way hierarchical agglomerative clustering applied to 79 genes (vertically) and to 7 left epicardial (Lepi) and left endocardial (Lendo), and 8 right epicardial (Repi) and right endocardial (Rendo; horizontally) samples
Same overall format as in Fig. 1.

Table 1. Tissue-related expression of Ca^{2+} channels, Na$^+$ channels and connexins

Subunit	RA	RV	PF
A. Calcium channels			
Cav1.2	647 ± 78	749 ± 116	455 ± 60
Cav1.3	7.7 ± 1.8	0.3 ± 0.1	1.2 ± 0.2
Cav3.1	20.6 ± 3.1	1.1 ± 0.3	4.3 ± 1.1
Cav3.2	7.4 ± 0.5	11.1 ± 1.6	8.9 ± 1.5
Cav$\alpha2\delta1$	234 ± 21	291 ± 24	283 ± 26
Cav$\alpha2\delta2$	188 ± 40	13.6 ± 2.2	30.7 ± 4.2
Cav$\beta2$	88.3 ± 18.0	89.4 ± 13.4	99.3 ± 12.5
B. Connexins			
Cx40	608 ± 186	177 ± 38	389 ± 71
Cx43	438 ± 60	898 ± 125	430 ± 53
Cx45	240 ± 22	226 ± 26	125 ± 9
C. Sodium channels			
Nav1.1	1.5 ± 0.5	2.7 ± 0.7	1.5 ± 0.5
Nav1.3	3.0 ± 0.7	7.1 ± 1.8	6.7 ± 1.2
Nav1.5	588 ± 53	731 ± 99	501 ± 51
Nav1.7	0.4 ± 0.1	1.4 ± 0.1	6.9 ± 0.7
Nav2.1	201 ± 32	286 ± 38	237 ± 46
Nav$\beta1$	622 ± 108	316 ± 63	397 ± 56
Nav$\beta2$	54.2 ± 6.9	91.1 ± 20.0	70.0 ± 18.6
Nav$\beta3$	6.2 ± 0.9	13.3 ± 1.3	12.3 ± 2.2

Abbreviations: RA, right atrium; RV, right ventricle; PF, Purkinje fibre. Units for all expression values are $2^{-\Delta Ct}$ *versus* reference gene ($\times 100$) expressed as means $\pm$ S.E.M.

Table 2. Tissue-related expression of Kv channel α-subunits and K$^+$ channel β-subunits

Subunit	RA	RV	PF
A. Kv channel α-subunits			
Herg	379 ± 40	400 ± 36	403 ± 56
Kv1.2	2.7 ± 0.4	4.1 ± 1.3	4.1 ± 1
Kv1.3	4.1 ± 1.0	1.6 ± 0.3	3.6 ± 0.4
Kv1.4	7.0 ± 1.8	34.0 ± 6.5	35.0 ± 3.8
Kv1.5	652 ± 112	26.1 ± 5.3	37.2 ± 10.4
Kv1.6	9.4 ± 0.7	3.5 ± 0.8	8.1 ± 1.0
Kv1.7	19.3 ± 4.9	13.9 ± 5.7	15.0 ± 1.1
Kv2.1	5.8 ± 3.1	8.9 ± 8.3	12.8 ± 1.4
Kv3.3	2.9 ± 0.4	1.7 ± 0.5	0.8 ± 0.2
Kv3.4	42.7 ± 2.3	30.0 ± 4.8	26.5 ± 2.4
Kv4.1	7.0 ± 0.9	4.0 ± 1.1	9.5 ± 1.7
Kv4.2	2.0 ± 0.7	1.5 ± 0.7	3.7 ± 1.0
Kv4.3	148 ± 20	91.0 ± 14.8	181 ± 20
KvLQT1	80.0 ± 9.8	116 ± 9	102 ± 5
B. K$^+$ channel β-subunits			
KChAP	44.3 ± 3.7	40.1 ± 1.4	66.8 ± 6.5
KChIP2	611 ± 83	704 ± 195	13.5 ± 4.0
Kv$\beta1$	14.9 ± 3.3	25.3 ± 3.3	12.7 ± 1.8
Kv$\beta2$	22.8 ± 3.6	46.7 ± 4.6	82.9 ± 10.0
Kv$\beta3$	0.2 ± 0.1	0.2 ± 0.1	2.4 ± 0.3
MinK	28.2 ± 4.1	21.5 ± 1.7	12.0 ± 0.4
MIRP1	2.3 ± 0.5	1.4 ± 0.4	3.0 ± 0.6
MIRP2	23.8 ± 2.1	23.9 ± 1.7	35.0 ± 7.1
MIRP3	57.5 ± 12.6	25.6 ± 4.5	34.5 ± 4.6
MIRP4	3.3 ± 0.5	2.4 ± 0.4	0.8 ± 0.2
SUR1	2.1 ± 0.3	1.7 ± 0.4	1.4 ± 0.3
SUR2	55.3 ± 5.9	99.6 ± 20.2	134 ± 11

Abbreviations: RA, right atrium ; RV, right ventricle; PF, Purkinje fibre. Units for all expression values are $2^{-\Delta Ct}$ *versus* reference gene ($\times 100$) expressed as means $\pm$ S.E.M.

RV, gene-expression are depicted in panels *A* of Figs 3–6. Only genes with significant differential expression between sets of matched atrial and ventricular samples from the same donors are shown.

Among the cardiac intertissue comparisons, the atria exhibited the most specific signature, including not only the largest number of differential genes (37/79 *versus* ventricle), but also the largest differences (relative expression up to 200-fold *versus* ventricles) in accordance with the microarray analysis of Barth *et al.* (2005). All of the genes that were responsible for the atrial *versus* ventricular sample clustering on hierarchical analysis (Cav1.3, Cav3.1, Cav$\alpha2\delta2$, Cx40, Nav$\beta1$, Kv1.3, Kv1.5, Kv1.6, MIRP3, Kir3.1, TWIK1, TASK1, HCN1 and HCN4) were statistically significantly more strongly expressed at the individual-transcript level in both atria. Another subunit that was more strongly expressed in both atria than corresponding ventricles was Kv4.3. Kir3.4, Kv4.2, SUR1, MIRP1 and MIRP4 were also more strongly expressed in atria than ventricles, but their absolute expression level was very low in all regions. Only three genes (Kir2.1, phospholamban and RyR2) exhibiting relatively high overall expression were more weakly expressed in atria than ventricles, and only one with overall low-level expression (Kv1.4). Although in many cases atrial-ventricular differences were seen for both sides of the heart, for some genes, significant atrial-ventricular expression differences were seen only for one atrium.

The specific molecular signature of non-diseased human Purkinje fibres

There are no data available in the literature regarding ion-channel gene expression in human Purkinje fibres, and only one paper characterizing Purkinje fibre ion-channel subunit expression in an animal model (Han *et al.* 2002*a*). Panels *B* in Figs 3–6 shows the statistically significant differences that we observed between human Purkinje fibres and RV. Among the 38 differentially expressed genes, 23 (60%) were more strongly expressed in Purkinje fibres. Seventeen ion-channel genes differentially expressed in Purkinje fibres were also similarly differentially expressed in atrium *versus* ventricle, indicating similarities between Purkinje fibre and atrial portraits. These particularly include Cav1.3, Cav3.1, Cav$\alpha2\delta2$, Cx40, Kv4.3, Kv1.3, Kir3.1, MiRP1, TWIK1, TASK1, HCN1 and HCN4

Table 3. Tissue-related expression of Kir channels, HCN channels and Cl⁻ channels

Subunit	RA	RV	PF
A. Kir channels			
Kir2.1	49.8 ± 7.3	201 ± 26	72.6 ± 10.2
Kir2.2	117 ± 25	125 ± 22	46.8 ± 6.6
Kir2.3	213 ± 41	106 ± 26	61.6 ± 10.8
Kir3.1	158 ± 24	3.9 ± 1.3	48.4 ± 9.2
Kir3.4	39.2 ± 6.8	20.4 ± 33.4	24.6 ± 5.9
Kir6.1	49.7 ± 7.6	158 ± 16	63.6 ± 9.8
Kir6.2	125 ± 19	172 ± 40	55.9 ± 4.5
TASK1	130 ± 34	8.9 ± 2.3	14.1 ± 2.1
TASK2	7.0 ± 1.6	5.3 ± 0.6	9.8 ± 1.8
TWIK1	745 ± 115	216 ± 31	350 ± 43
B. HCN channels			
HCN1	70.3 ± 9.6	0.4 ± 0.1	8.2 ± 3.1
HCN2	159 ± 41	24.7 ± 6.0	11.4 ± 2.3
HCN3	4.2 ± 0.7	5.7 ± 1.6	8.9 ± 1.2
HCN4	214 ± 32	75.9 ± 17.9	98.2 ± 11.1
C. Chloride channels			
ClC2	10.7 ± 1.2	13.2 ± 1.1	18.6 ± 2.8
ClC3	130 ± 11	153 ± 21	95.3 ± 4.0
ClC6	132 ± 11	146 ± 12	175 ± 18
ClC7	160 ± 19	183 ± 34	164 ± 20

Abbreviations: RA, right atrium; RV, right ventricle; PF, Purkinje fibre. Units for all expression values are $2^{-\Delta C_t}$ *versus* reference gene ($\times 100$) expressed as means $\pm$ S.E.M.

Table 4. Tissue-related expression of pumps, exchangers and calcium handling subunits

Subunit	RA	RV	PF
A. Pumps and exchangers			
Na/K ATPase $\alpha 1$	1010 ± 232	1272 ± 201	1502 ± 265
Na/K ATPase $\alpha 3$	4100 ± 167	5446 ± 526	1345 ± 195
Na/K ATPase $\beta 1$	1519 ± 97	2219 ± 188	1631 ± 138
NCX1	1401 ± 55	2208 ± 278	1189 ± 139
PMCA1	48.7 ± 6.2	54.7 ± 4.3	55.8 ± 5.7
PMCA4	720 ± 76	874 ± 128	934 ± 146
SERCA2	7801 ± 746	8696 ± 840	2687 ± 194
SERCA3	79.2 ± 6.5	61.4 ± 4.4	81.4 ± 13.7
B. Calcium handling and signalling			
CALM1	123 ± 11	182 ± 8	478 ± 38
CALM3	1017 ± 56	1349 ± 119	1299 ± 79
CAM-PRP	63.1 ± 6.3	86.9 ± 9.7	71.9 ± 9.2
CASQ1	96.8 ± 26.3	130 ± 29	157 ± 35
CASQ2	3524 ± 286	4147 ± 416	1916 ± 236
InsP3R1	117 ± 12	153 ± 16	246 ± 26
InsP3R3	69.5 ± 7.9	106 ± 19	131 ± 16
PLB	4703 ± 871	9519 ± 1008	7622 ± 1343
RYR2	12940 ± 1352	25054 ± 2571	8612 ± 397

Abbreviations: RA, right atrium; RV, right ventricle; PF, Purkinje fibre. Units for all expression values are $2^{-\Delta C_t}$ *versus* reference gene ($\times 100$) expressed as means $\pm$ S.E.M.

(expression stronger than in ventricle) and Cx43, Kir2.1 and Kir6.1 (weaker than in ventricle). Differences specific to Purkinje fibres (i.e. not seen in atria) were much weaker expression of KChIP2 (-96% *versus* ventricle), weaker expression of Kir2.2 and Kir6.2 and stronger expression of Nav1.7, KChAP and HCN3. Differences in Ca^{2+}-regulation genes also characterized Purkinje fibres *versus* ventricular myocardium, including stronger Purkinje fibre expression of CALM1, InsP3R1 and InsP3R3 and weaker expression of Na^+,K^+-ATPase $\alpha 3$, SERCA2, CASQ2, RyR2 and NCX1.

The specific molecular signature of non-diseased human epicardium *versus* endocardium

In a fashion similar to our analysis of atrial–ventricular differences, we analysed endocardium–epicardium differences in a chamber side-specific way, i.e. LV epicardium *versus* endocardium and RV epicardium *versus* endocardium, using matched samples from each heart. Only 10 genes were identified as statistically differing between epi- and endocardium for both right and left sides (panels *C* in Figs 3–6). Further, the relative differences between epicardium and endocardium were smaller compared to other interregional differences. As expected, KChIP2 exhibited the strongest transmural gradient, with $\sim$51-fold stronger expression in left epicardium *versus* left endocardium. For both Lepi and Repi, Cav1.2, SERCA2, CALM3 and calcineurin-α transcripts were concordantly more strongly expressed. Conversely, Nav1.5, Nav$\beta 1$, Kv1.4 and Kir3.1 were more strongly expressed in the endocardium. Some genes showed differential epicardial-endocardial expression only on the right side (Cav3.1, Kir2.2, Kv4.2 and RYR2 were more strongly expressed in epicardium, Kv$\beta 2$ and Kir2.1 in endocardium). Similarly, KvLQT1, Kir6.1 and NCX1 were more strongly expressed in left epicardium *versus* endocardium, whereas Cav$\alpha 2\delta 1$, Cx40, Nav2.1, Kv1.5, TASK1, TASK2, HCN2, Na^+,K^+-ATPase $\alpha 1$ and InsP3R1 showed stronger expression in left endocardium.

Protein correlates

Western-blot experiments were conducted to relate protein expression to that of mRNA for selected ion-channel sub-units. Figure 7 (left panels) shows original blots (4 samples for LA, LV, LV epicardium and LV endocardium all run on the same gel), as well as overall mean data (right panels). In agreement with transcriptional data, Cav1.3, Kv1.5, Kv4.3, KChIP2, TWIK1 and Cx40 were more strongly expressed in atria *versus* ventricular compartments. Cx40 and Kv1.5 expressed at very low levels in both ventricular endocardium and epicardium, whereas KChIP2 was more strongly expressed in epicardium. In general, protein expression was in good agreement with qRT-PCR results.
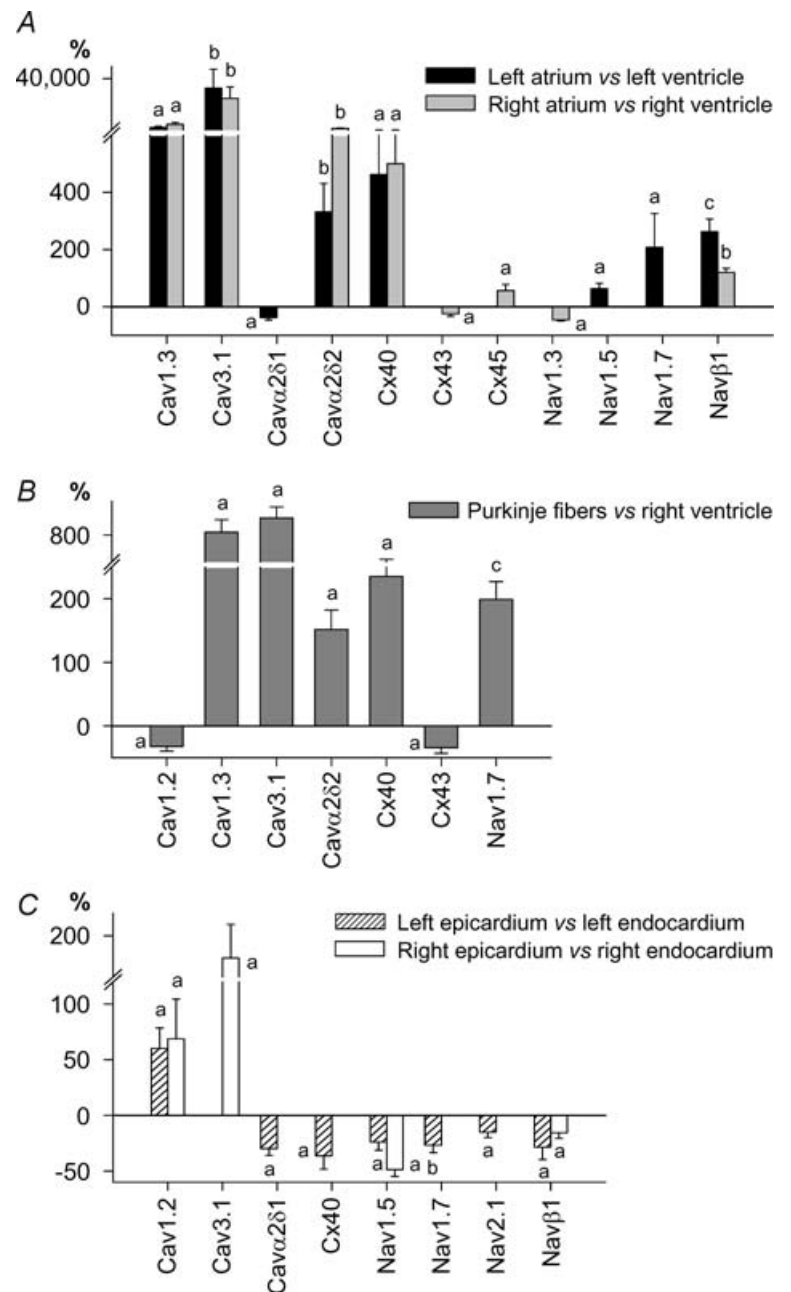
Discussion

We have performed the first detailed analysis of regional ion-channel gene expression in the non-diseased human heart. Our study shows that human atria, ventricles and Purkinje fibres show distinct patterns of ion-channel and transporter expression. The intertissue differences are much greater than differences between left- and right-sided chambers and between endocardium and epicardium, which do not show distinct clustering on hierarchical analysis.

The challenge of ion-channel expression profiling and human cardiac spatial electrophysiological heterogeneity

The importance of regional heterogeneity in cardiac ion-channel function is well-recognized (Schram *et al.* 2002; Antzelevitch, 2004). Most previous studies have examined the molecular basis by quantifying the expression of limited numbers (generally 5 or fewer) of ion-channel genes and/or proteins in selected regions, e.g. right *versus* left atrium (Li *et al.* 2001), endocardium

Figure 3. Expression profile of Ca^{2+} channels, connexins and Na$^+$ channels in the human heart
Differentially expressed genes in atria *versus* ventricles (*A*), in Purkinje fibres *versus* RV (*B*) and in epicardium *versus* endocardium (*C*). Data are expressed as percentage difference. a, $P < 0.05$; b, $P < 0.01$; and c, $P < 0.001$.

versus epicardium (Brahmajothi *et al.* 1999; Rosati *et al.* 2001; Zicha *et al.* 2004; Yamada *et al.* 2004) and atria *versus* ventricles (Melnyk *et al.* 2002). A problem with this approach is that only a limited number of subunits are assessed, usually including primarily subunits for which spatial heterogeneity is expected. Thus, the relative expression levels of these subunits compared to the overall spectrum of cardiac ion-channel subunits is unknown, subunits that may have important but unsuspected regional variability are not assessed, and a very limited range of ion channel function is examined. An emerging alternative approach is to establish a more global expression portrait with genomic methodology. Understanding ion-channel distribution in the human heart is clearly of great physiological and clinical importance, but

presents additional difficulties in terms of the paucity of tissue sample availability, particularly for non-diseased human cardiac tissue. Genomic methodology has the additional advantage of obtaining a maximum amount of information from limited samples, like those available from non-diseased human hearts.

Most previous large-scale studies of regional cardiac gene expression have used microarray-based profiling with pan-genomic arrays. Pan-genomic arrays are limited in their ability to detect differences in low-abundance gene products like those of most cardiac ion-channel subunits. In this study, we used high-throughput quantitative RT-PCR for a comprehensive panel of human cardiac ion channel and transporter subunit genes. This method has the advantages of being sensitive, specific
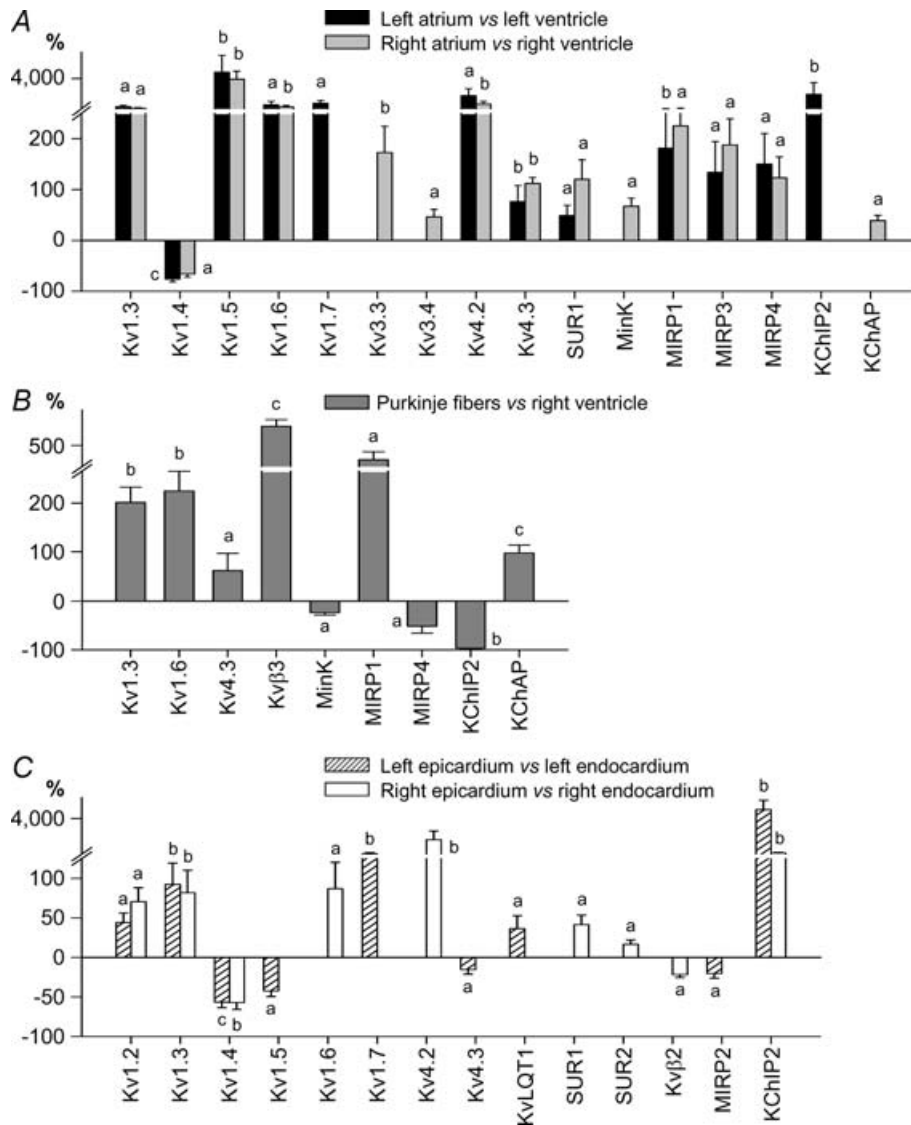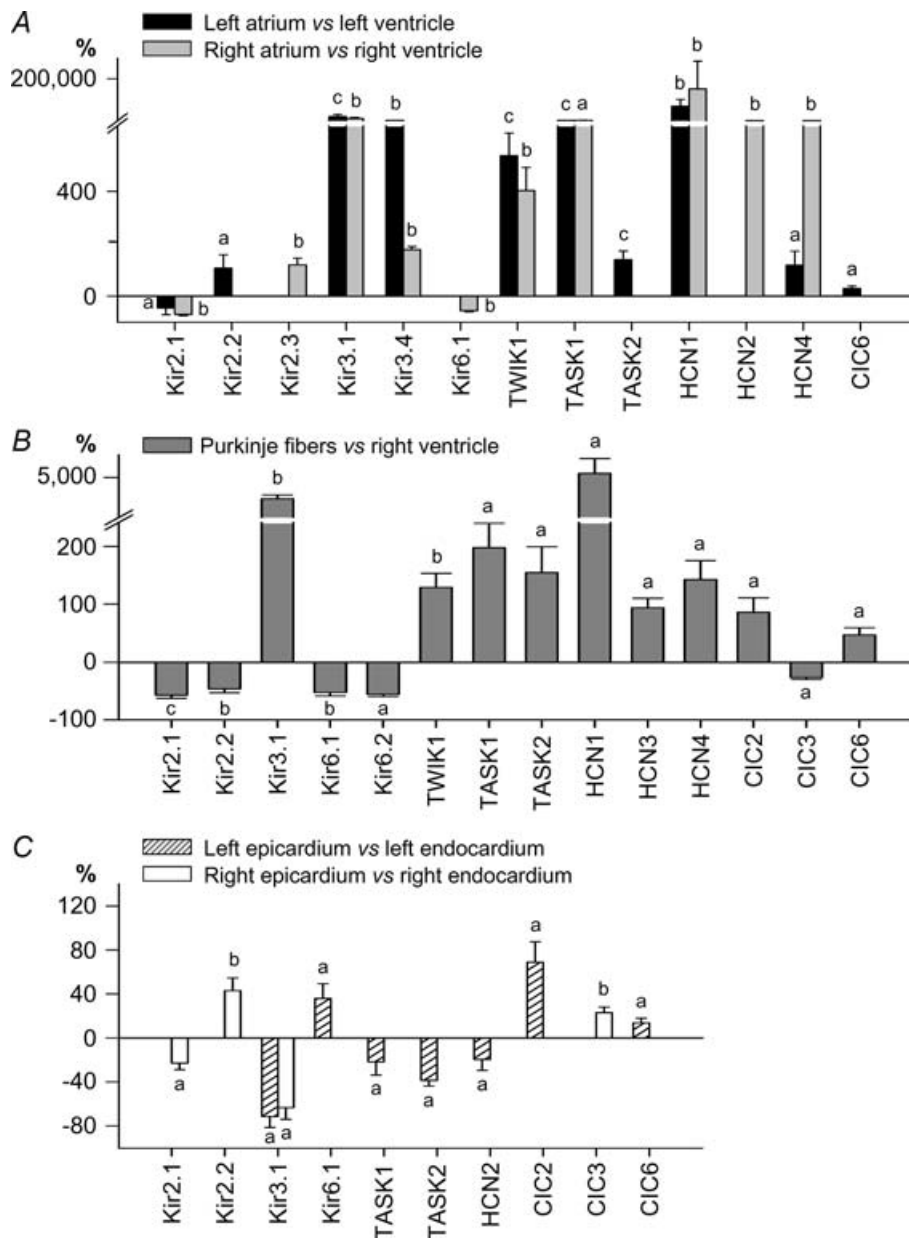

Figure 4. Expression profile of K$^+$ channel α- and β-subunits in the human heart
Same presentation and symbols as in Fig. 3.

and quantitative, and not requiring validation by other methods. Consequently, we were able to obtain a much more detailed regional ion-channel expression profile than previous studies. For example, Ellinghaus *et al.* (2005) described four human ion-channel genes with differential atrial–ventricular expression (Kv1.5, Kir2.1, TWIK1, TASK1) and Barth *et al.* (2005) described three such genes (Kir2.3, TWIK1, TWIK3) with the use of pan-genomic arrays, in contrast to the 24 we identified. Rosati *et al.* (2006) used pan-genomic arrays to study epicardial-endocardial gene-expression differences in rat hearts, identifying Nav1.5 and Kv4.2

as differentially expressed. We observed corresponding differences in Nav1.5 and KChIP2 (responsible for endocardial-epicardial I_{to} differences in mammalian hearts), but were also able to identify robust differential expression of nine other ion channel or transporter subunits.

Our approach differs from previous studies in that we analysed tissue compartments that have, to our knowledge, not previously been studied by wide-scale gene profiling (e.g. Purkinje fibres, right *versus* left sided atrium/ventricle and epicardium/endocardium). This is also to our knowledge the first study to apply

Figure 5. Expression profile of Kir, HCN and Cl⁻ channels in the human heart
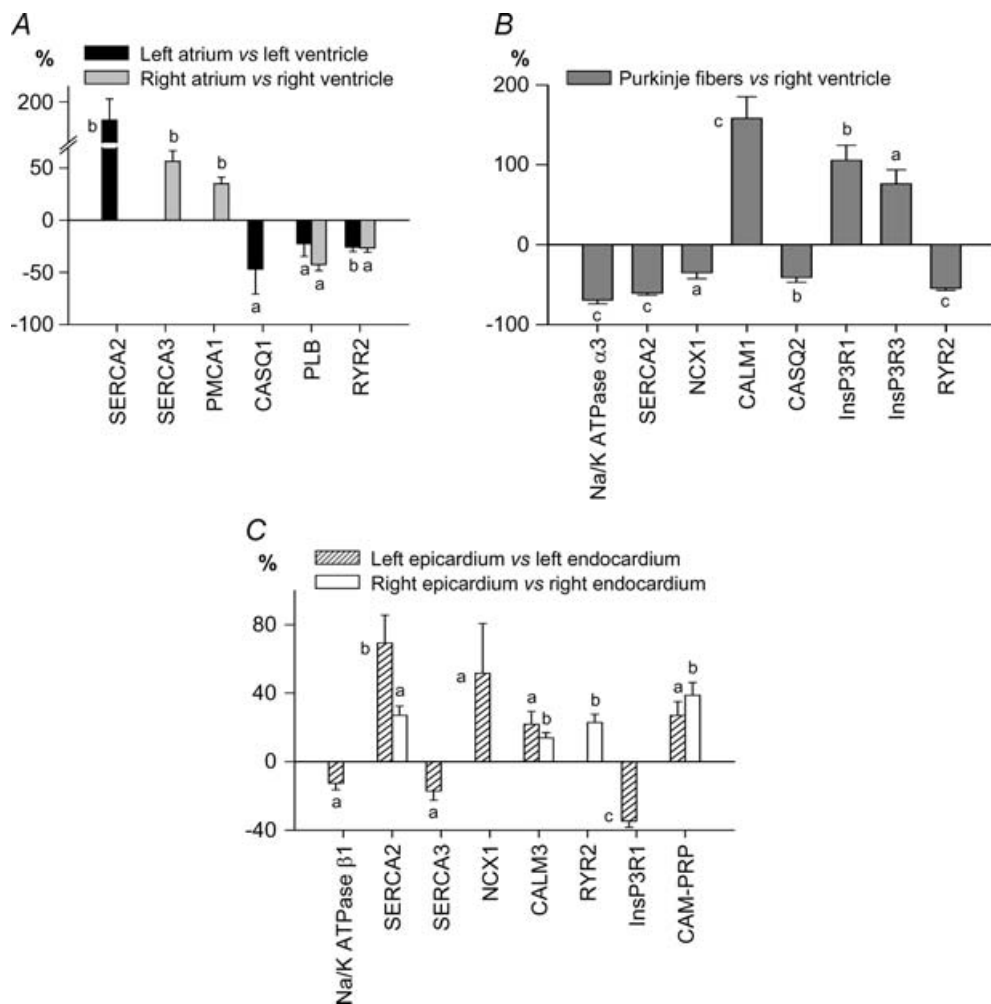Same presentation and symbols as in Fig. 3.

gene-expression profiling simultaneously to such a large number of regional compartments, allowing us to compare the relative contributions of diverse regional factors within the same hearts. The use of apparently normal human hearts adds to the novelty and potential impact of our study.

Compatability with previously available information on regional ion-channel subunit expression variations and functional relevance

Among the differences that we observed, many are consistent with functionally relevant information in the previous literature and provide a useful confirmation of the validity of our approach. With respect to Ca^{2+}-channel subunits, the predominant atrial expression of Cav1.3 has previously been reported in mouse, rabbit and human hearts (Mangoni *et al.* 2003; Marionneau *et al.* 2005; Qu *et al.* 2005). Among Na^+-channel subunits, Nav1.5

and Navβ1 showed stronger endocardial *versus* epicardial expression, similar to a recent report in rat hearts (Rosati *et al.* 2006) and to observations that I_{Na} density is larger in rat and canine endocardium *versus* epicardium (Ashamalla *et al.* 2001; Ueda *et al.* 2004b).

With respect to K^+-channel subunits, our findings are consistent with several known differences with great functional significance. Similar to Rosati *et al.* (2001, 2003), we found that KChIP2 is one of a small number of genes showing a strong epicardial–endocardial gradient, of great functional importance with respect to clinically relevant transmural repolarization gradients (Antzelevitch, 2004; Nabauer *et al.* 1996). The higher-level atrial *versus* ventricular expression levels of Kv1.5, TWIK1 and TASK1, and the lower atrial levels of Kir2.1, are consistent with previous observations of Ellinghaus *et al.* (2005). Kv1.5 encodes an important human atrial K^+-channel that is an interesting potential target for new antiarrhythmic drug development (Nattel

Figure 6. Expression profile of pumps, exchangers and Ca^{2+} handling proteins in the human heart
Same presentation and symbols as in Fig. 3.

et al. 1999). TWIK1 and TASK1 encode two-pore background K^+-channels with currently unclear but potentially substantial physiological importance (Duprat *et al.* 1997; Gaborit *et al.* 2005). Stronger ventricular Kir2.1 expression correlates with the more negative ventricular-myocyte resting potential (Schram *et al.* 2002) and the ventricular-selective arrhythmogenic consequences of Kir2.1 mutations in Andersen's syndrome (Plaster *et al.* 2001). The α-subunit Kv1.4 associated with the slow component, I_{tos}, is more abundant in the endocardium, in agreement with studies showing larger I_{tos} in endocardial cells (Kaab & Nabauer, 2001). Predominant atrial expression was previously found for HCN4 in humans and for HCN1 and HCN4 in the mouse (Ueda *et al.* 2004*a*; Marionneau *et al.* 2005), observations related to the pacemaking contribution of the I_f channels they encode (Thuringer *et al.* 1992; Michels *et al.* 2005).

The dominant epicardial expression of Cav1.2 is associated with preferential expression of RyR2, consistent with specific contractile properties of epicardium. Human epicardial cells display faster onset and peak of contraction than endocardial cells (Fulop *et al.* 2004). Epicardial cells also exhibit faster relaxation (Cordeiro *et al.* 2004). In agreement with these functional observations and previous findings (Prestle *et al.* 1999; Xiong *et al.* 2005), we observed that the sarcoplasmic-reticulum calcium-ATPase 2 (SERCA2) and Na^+/Ca^{2+} exchanger responsible for cytoplasmic Ca^{2+} removal are predominantly expressed in the epicardium. Particularly strong inositol trisphosphate receptor ($InsP_3R$) expression in Purkinje fibres is consistent with prior protein and *in situ* hybridization studies (Gorza *et al.* 1993), and may be important because of the emerging role of $InsP_3Rs$ in arrhythmias (Li *et al.* 2005).
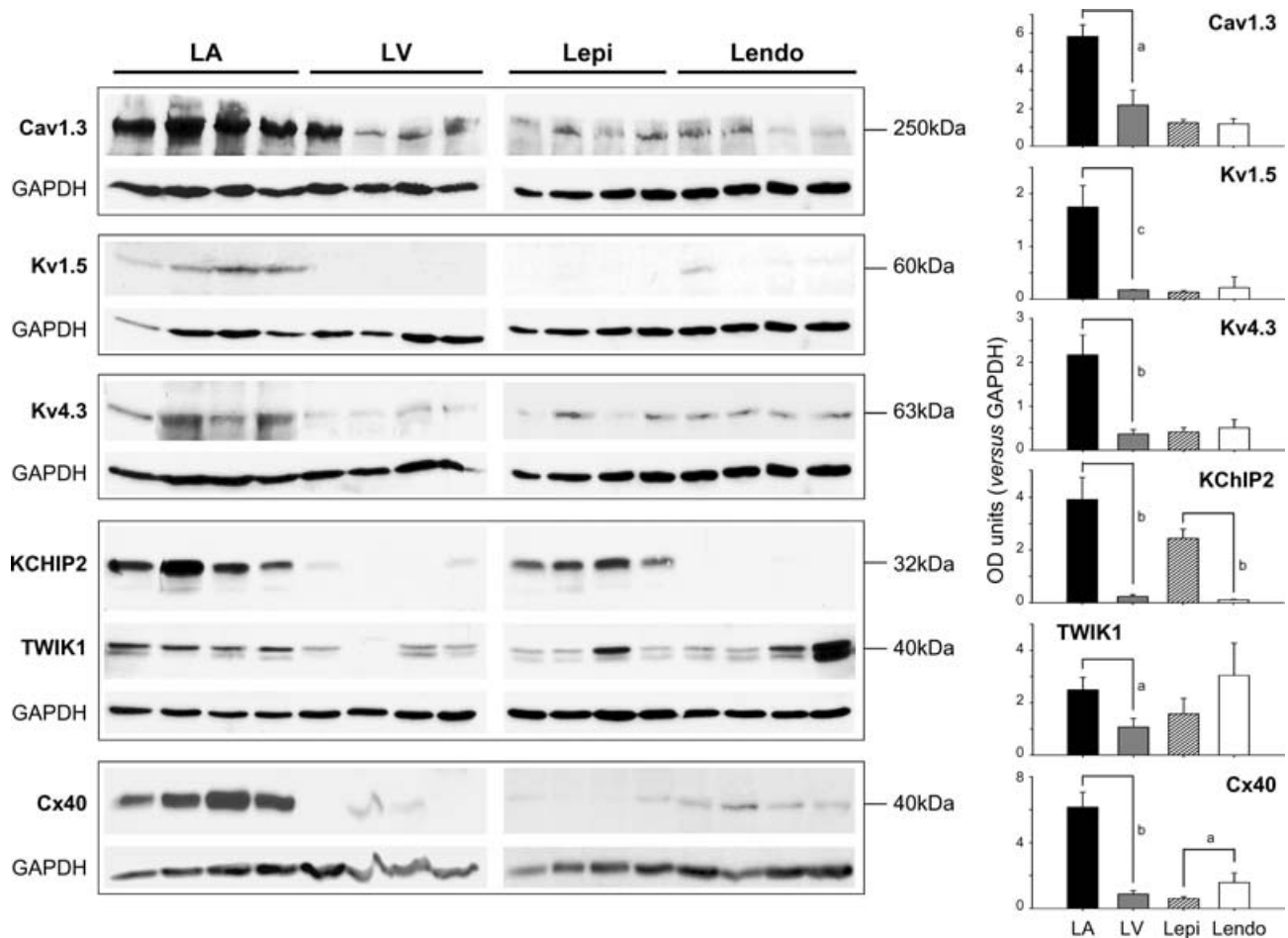
Figure 7. Western-blot analysis of key channel proteins
Left, representative Western blots probed with anti-Cav1.3, anti-Kv1.5, anti-Kv4.3, anti-KChIP2, anti-TWIK1 and anti-Cx40 antibodies. GAPDH is shown as loading control. Expected molecular masses are indicated. Right, mean ± s.e.m. ion-channel subunit protein expression values normalized to that of GAPDH. a, $P < 0.05$; b, $P < 0.01$; and c, $P < 0.001$ for LA *versus* LV and for Lepi *versus* Lendo, $n = 4$ tissue samples per group.

It should be noted that not all of our findings were confirmatory. For example, the largest previous study of ion channel gene expression in cardiac Purkinje fibres noted lower-level expression of KvLQT1, HERG, KChIP2 and Cav1.2 mRNA, along with higher-level Kv3.4, Cav3.1, 3.2, 3.3 and HCN4, in canine Purkinje fibres compared to ventricular muscle (Han *et al.* 2002*a*). In addition, NCX1 protein was less strongly expressed in Purkinje fibres. In the present investigation, we observed lower-level transcript expression of KChIP2, Cav1.2 and NCX1, and higher-level Cav3.1 and HCN4, in human Purkinje fibres *versus* ventricular muscle. Our results confirm stronger HCN4 expression as a candidate mechanism for Purkinje fibre automaticity and weaker KChIP2 as an explanation for more slowly recovering Purkinje-fibre I_{to}. However, they leave open the mechanism for tetraethylammonium sensitivity of Purkinje I_{to} (previously suggested to be related to higher-level Kv3.4) and longer action potential duration (previously related to lower-level delayed-rectifier channel subunit expression). Rosati *et al.* (2007) recently reported several hundred-fold greater expression of Cav3.2 *versus* Cav3.1 in canine Purkinje fibres, whereas in the present study they were of the same order. The discrepancies may be due to species differences or to methodological issues. Because of the large number of observations in the present study, it would be impossible to catalogue all of the similarities and differences between the present findings and previous observations in the literature, but we have attempted to provide illustrative confirmatory observations of physiological significance as well as some potentially significant discrepancies.

Novel findings of potential functional significance

Because of the comprehensive and quantitative nature of our approach, a number of potentially significant and novel findings, many of them not predictable a priori, have emerged. They will be discussed in relation to specific tissue compartments and to overall regional ion-channel gene-expression profiles.

Atrium. Na$^+$ current in human atrial cells has some specific inactivation properties not seen in ventricular tissue (Sakakibara *et al.* 1992). These may relate to the high-level expression and differential atrial distribution of the Navβ1 subunit (Makita *et al.* 1994) that we observed. We found high levels of Cav$\alpha2\delta2$ in the atria, which were ~12- and 6-fold greater than in ventricle and Purkinje tissue, respectively. This subunit, which importantly modulates currents expressed by Cav1.2, 1.3 and 3.1 subunits (Gao *et al.* 2000), is therefore a likely contributor to atrial-specific properties of L- and T-type Ca^{2+}-currents.

We have obtained the first detailed comparison of putative I_{to}-forming subunits (Kv1.4, Kv4.3, Kv4.2 and KChIP2) in human atria *versus* ventricles. Kv4.3, the predominant I_{to} α-subunit, was expressed significantly more strongly in atrium than ventricle, potentially accounting (at least in part) for previously described functional and pharmacological differences between atrial and ventricular I_{to} (Nattel *et al.* 2000; Varro *et al.* 1993).

Purkinje fibres

The largest mass of new information emerging from the present study concerns cardiac Purkinje fibres. There are no previous data in the literature regarding ion-channel expression in human cardiac Purkinje fibres. Furthermore, the available information regarding Purkinje fibre ion-channel function and subunit expression is extremely limited, despite the substantial significance of Purkinje tissue in cardiac electrical function and arrhythmias (Schram *et al.* 2002).

Purkinje fibre I_{Na} displays tetrodotoxin (TTX) sensitivity, which is not shared with ventricular I_{Na} (Carmeliet, 1987) and is currently unexplained. Neuronal Nav1.7 subunits are TTX sensitive (Klugbauer *et al.* 1995) and were expressed ~5- to 10-fold more strongly in human cardiac Purkinje fibres *versus* right atrium and ventricle, providing a potential explanation.

Transcripts encoding a variety of proteins involved in Ca^{2+} handling or coupled functions, including the principal Na$^+$,K$^+$-ATPase isoforms $\alpha3$ and $\beta1$, NCX1, SERCA2, CASQ2 and RYR2, were expressed at substantially lower (27–75%) levels in Purkinje fibre *versus* ventricular muscle tissue, compatible with the limited contractile function of Purkinje fibres (Schram *et al.* 2002). Purkinje fibres classically display enhanced sensitivity to digitalis toxicity, despite reduced ouabain binding (Rhee, 1981). The low-level Purkinje-fibre Na$^+$,K$^+$-ATPase expression that we observed is likely to account for this previously puzzling finding, since Na$^+$,K$^+$-ATPase is both the functional target and receptor for digitalis.

We found Kv4.3-subunit expression to be abundant in human Purkinje fibres, whereas KChIP2 was sparse, consistent with the very slow recovery of human Purkinje fibre I_{to} from inactivation (Han *et al.* 2002*b*). Conversely, KChAP is more strongly expressed in Purkinje fibres than ventricular muscle and predominates over KChIP2. KChAP acts as a chaperone to enhance expression and current density of a subset of Kv channels, including Kv4.3 (Kuryshev *et al.* 2000). KChAP has not yet been shown to have a physiological role in ventricular tissue, but our results suggest the possibility that KChAP may participate in Purkinje fibre I_{to}. Consistent with previous findings in dogs (Pourrier *et al.* 2003), we found stronger expression of MiRP1 in Purkinje fibres than in ventricles,

pointing to a possible role of Purkinje tissue in human arrhythmia syndromes associated with MiRP1 mutations (Abbott *et al.* 1999). Functional evidence suggests the absence of Kv1.5-based currents in human Purkinje fibres (Han *et al.* 2002*b*), paralleling previous observations for human ventricular muscle (Feng *et al.* 1997). Our observation of ~20-fold lower expression levels of Kv1.5 in human Purkinje tissue *versus* atrium provides the first molecular data indicating atrial-selective expression of this subunit compared to Purkinje tissue. This finding is potentially important in view of the therapeutic interest of atrial-selective ion-channel blockade in atrial fibrillation (Goldstein & Stambler, 2005) and continuing controversy regarding the atrial-selective expression of Kv1.5-based currents (Sridhar *et al.* 2006). Lower Purkinje Kir2.x expression *versus* ventricular muscle is consistent with the smaller I_{K1} observed in Purkinje fibres (Verkerk *et al.* 1999). An acetylcholine-dependent K^+-current (I_{KACh}) has been described in rabbit Purkinje fibres (Carmeliet & Mubagwa, 1986) and stimulation of muscarinic receptors

in canine Purkinje fibres reduces action potential duration (Malfatto *et al.* 1996), in contrast to the lack of I_{KACh} in ventricular muscle and consistent with our observation of substantially greater Kir3.1 expression in Purkinje tissue.

Overall interregional differences

One advantage of the type of broadly based expression analysis approach that we took is that it allows for the development of portraits of regionally specific gene expression. Figure 8 summarizes a number of regional expression portraits of interest. The absolute expression level of more strongly expressed genes in the region of interest is provided by colour coding: genes expressed > 20-fold the reference gene (*HPRT*) are indicated in bold and genes expressed at > 185 times the reference gene level are shown in red. Atrial-selective gene expression (*versus* ventricular) is shown for only the most robust differences, i.e. genes showing statistically significant differential
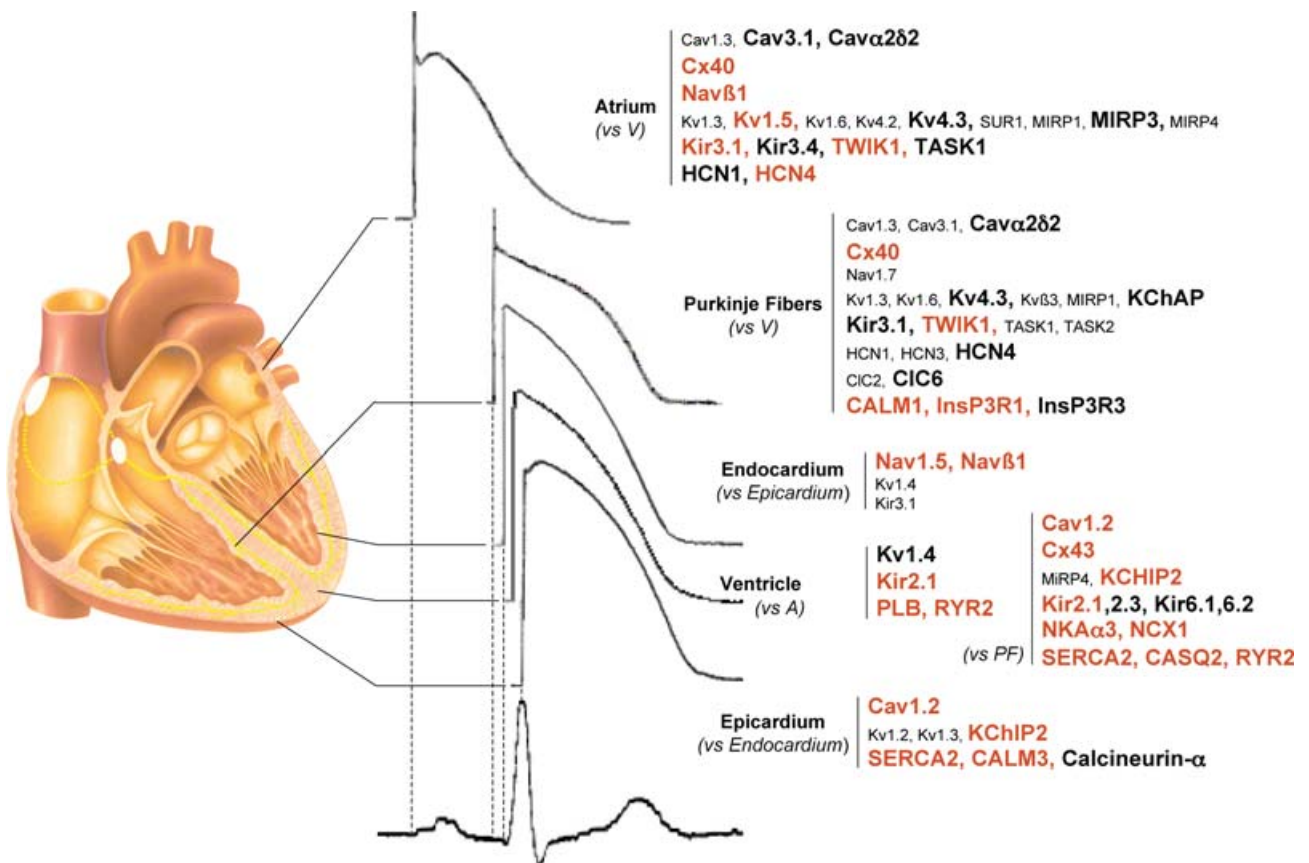
Figure 8. Schematic diagram of the heart illustrating statistically significant gene-expression differences that create an ion-channel 'signature' for various cardiac regions
The absolute expression levels of genes that are significantly more strongly expressed in a region of interest relative to the reference region indicated are provided by colour coding: genes expressed > 20-fold the reference gene (*HPRT*) in the tissue/region of interest are indicated in bold and genes expressed at > 185 times the reference gene level are shown in bold red. Values shown are differences that were statistically significant for both right and left-sided comparisons for atrium *versus* ventricle and epicardium *versus* endocardium.

expression in the same direction for both RA *versus* RV and LA *versus* LV. Of note, the atrial gene-expression signature shares many properties with that of Purkinje fibres. Of the 20 genes that are significantly different for atrium *versus* ventricle, 12 (60%) show the same directional statistically significant difference for Purkinje tissue *versus* ventricle. The basis for this similarity in ion-channel subunit expression between atrium and Purkinje fibres is unclear, but may relate to the strong contractile phenotype of working ventricular myocardium. One general difference between atrium and Purkinje tissue pertains to Ca^{2+}-homeostasis proteins, which are much more strongly expressed in the atrium (as in the ventricles) compared to Purkinje tissue, possibly reflecting the primarily electrical (and non-contractile) specialization of the Purkinje system. The second difference lies in the weaker expression of Na^+,K^+-ATPase and stronger expression of inositol trisphosphate receptor genes in Purkinje fibres, which may be related to some of their specific arrhythmic properties.

We did not observe statistically significant overall gene expression clustering between right and left sided chambers or between ventricular epicardium and endocardium. This finding suggests that tissue differences (i.e. atrium *versus* ventricle *versus* Purkinje fibres) are much stronger determinants of ion-channel subunit expression pattern than regional differences. We were careful to analyse atrial–ventricular and epicardial–endocardial differences with matched samples for right *versus* left sided chambers. To our knowledge, this is the first time that an extensive analysis of this type has been performed. Despite the overall lack of distinct gene clustering for endocardium *versus* epicardium, there were specific differences (illustrated in Fig. 8) that appeared to be robust in that they were statistically different and in the same direction for both right epicardium *versus* endocardium and left epicardium *versus* endocardium. The endocardial gene-expression pattern is marked by stronger Na^+-channel subunit expression, potentially reflecting a need for more rapid endocardial conduction. That this difference is not due to contamination by subendocardial Purkinje tissue is apparent by virtue of the lack of differential expression of the same subunits for Purkinje tissue *versus* ventricle. The epicardial expression pattern is marked by enhanced expression of genes related to Ca^{2+} handling (Cav1.2 and SERCA2), Ca^{2+} signalling (calmodulin and calcineurin) and I_{to} (KChIP2), which is believed to be an important regulator of Ca^{2+} entry, Ca^{2+} signalling and contractility (Sah *et al.* 2003; Lebeche *et al.* 2004).

Study limitations

Transcripts do not necessarily translate into functional proteins and although transcriptional regulation of

ion-channel expression is a key regulatory mechanism (Rosati & McKinnon, 2004), translational and post-translational processes are also important. We confirmed corresponding changes for selected proteins of interest, but no technology is currently available to explore on a large scale the expression of a collection of membrane proteins such as those corresponding to the 79 genes we studied. For Western blot analyses, we selected proteins for study in order to contrast atrial with ventricular and epicardial with endocardial expression. All of the subunits selected had evidence for substantial atrial–ventricular mRNA differences, and two of them (KChIP2 and Cx40) significant endocardial–epicardial differences. This allowed us to test the specific hypothesis that A–V and Epi–Endo differences apparent with RT-PCR are also reflected in protein differences. In addition, Cav1.3, Kv1.5 and Cx40 are all important in the pathogenesis of atrial fibrillation (the most important clinical atrial electrical rhythm disturbance). TWIK1 was very strongly expressed as determined by RT-PCR, suggesting possible functional importance despite poorly understood physiology, so we felt that it would be worthwhile to determine whether protein differences parallel those in mRNA, supporting the potential relevance of the mRNA data for TWIK1.

Another limitation relates to the location of sampling. Heterogeneous expression exists within the different parts of the atrium and the base and apex of the ventricle. However, it is encouraging to note that atrial–ventricular–Purkinje fibre differences were much greater than those between right- and left-sided cavities or endocardium *versus* epicardium, suggesting that inter-tissue differences are likely to be robust across within-tissue regions. Finally, targeting of ion channel proteins to subcellular compartments is crucial for their function and cannot be approached by our global analysis. Despite these limitations, genomics represents a powerful means to improve our understanding of the complex mechanisms used by heart muscle to adapt to different functional requirements in diverse cardiac tissues and regions.

We cannot totally exclude the contamination of endocardial samples by subendocardial Purkinje fibre cells. However, the mass of the thin subendocardial Purkinje tissue layer is relatively small compared to that of underlying ventricular muscle. More importantly, important contamination seems unlikely based on the gene expression data themselves. For example, Kv1.4, Nav1.5 and Navβ1 are more strongly expressed in endocardium than epicardium, but these subunits were in fact not significantly more strongly expressed in Purkinje fibres than in ventricular muscle. If contamination of subendocardial muscle samples by Purkinje tissue were to account for the greater expression of these subunits in endocardium, they would have had to be expressed more strongly in pure Purkinje fibre tissue (like false tendons) than in ventricular muscle.

We examined a limited range of cardiac regions. There are many interesting additional regional differences in electrophysiological function that would be appropriate subjects for detailed expression-profiling analysis, e.g. apex *versus* base *versus* septum, various right atrial regions with distinct electrical function (pectinate muscles, AV ring, crista terminalis, appendage), various left atrial regions (pulmonary vein ostia, free wall, appendage), Bachmann's bundle, the nodes, etc. Practical considerations (time constraints, financial resources, tissue availability, etc.) precluded their inclusion in the present study but they are certainly an appropriate subject for future investigation.

Conclusions

This work has elucidated the regional expression of a large number of ion-channel subunit genes in the non-diseased human heart. We found unique ion channel and transporter subunit transcript expression signatures among atrial, working ventricle and Purkinje fibre compartments, in contrast to epicardial–endocardial and right–left chamber differences, which showed no distinct pattern on hierarchical clustering. This first detailed analysis that specifically and simultaneously characterizes the expression of a broad range of ion channel and transporter genes in multiple tissue compartments of the non-diseased human heart has significant potential implications for understanding regional electrophysiology, arrhythmia mechanisms, and responses to ion-channel blocking drugs. In addition, this study lays the groundwork for future investigations seeking to elucidate how ionic remodelling caused by heart disease alters the regional specificity of subunit expression and for studies of the functional importance of a number of currently poorly characterized subunits that show strong and/or highly differential regional expression.

References

Abbott GW, Sesti F, Splawski I, Buck ME, Lehmann MH, Timothy KW, Keating MT & Goldstein SA (1999). MiRP1 forms IKr potassium channels with HERG and is associated with cardiac arrhythmia. *Cell* **97**, 175–187.

Antzelevitch C (2004). Cellular basis and mechanism underlying normal and abnormal myocardial repolarization and arrhythmogenesis. *Ann Med* **36**, 5–14.

Ashamalla SM, Navarro D & Ward CA (2001). Gradient of sodium current across the left ventricular wall of adult rat hearts. *J Physiol* **536**, 439–443.

Barth AS, Merk S, Arnoldi E, Zwermann L, Kloos P, Gebauer M, Steinmeyer K, Bleich M, Kaab S, Pfeufer A, Uberfuhr P, Dugas M, Steinbeck G & Nabauer M (2005). Functional profiling of human atrial and ventricular gene expression. *Pflugers Arch* **450**, 201–208.

Brahmajothi MV, Campbell DL, Rasmusson RL, Morales MJ, Trimmer JS, Nerbonne JM & Strauss HC (1999). Distinct transient outward potassium current (Ito) phenotypes and distribution of fast-inactivating potassium channel α subunits in ferret left ventricular myocytes. *J Gen Physiol* **113**, 581–600.

Carmeliet E (1987). Voltage-dependent block by tetrodotoxin of the sodium channel in rabbit cardiac Purkinje fibers. *Biophys J* **51**, 109–114.

Carmeliet E & Mubagwa K (1986). Desensitization of the acetylcholine-induced increase of potassium conductance in rabbit cardiac Purkinje fibres. *J Physiol* **371**, 239–255.

Cordeiro JM, Greene L, Heilmann C, Antzelevitch D & Antzelevitch C (2004). Transmural heterogeneity of calcium activity and mechanical function in the canine left ventricle. *Am J Physiol Heart Circ Physiol* **286**, H1471–H1479.

DePaoli AM, Bell GI & Stoffel M (1994). G protein-activated inwardly rectifying potassium channel (GIRK1/KGA) mRNA in adult rat heart and brain by in situ hybridization histochemistry. *Mol Cell Neurosci* **5**, 515–522.

Dhamoon AS, Pandit SV, Sarmast F, Parisian KR, Guha P, Li Y, Bagwe S, Taffet SM & Anumonwo JM (2004). Unique Kir2.x properties determine regional and species differences in the cardiac inward rectifier K^+ current. *Circ Res* **94**, 1332–1339.

Duprat F, Lesage F, Fink M, Reyes R, Heurteaux C & Lazdunski M (1997). TASK, a human background K^+ channel to sense external pH variations near physiological pH. *EMBO J* **16**, 5464–5471.

Eisen MB, Spellman PT, Brown PO & Botstein D (1998). Cluster analysis and display of genome-wide expression patterns. *Proc Natl Acad Sci U S A* **95**, 14863–14868.

Ellinghaus P, Scheubel RJ, Dobrev D, Ravens U, Holtz J, Huetter J, Nielsch U & Morawietz H (2005). Comparing the global mRNA expression profile of human atrial and ventricular myocardium with high-density oligonucleotide arrays. *J Thorac Cardiovasc Surg* **129**, 1383–1390.

Feng J, Wible B, Li GR, Wang Z & Nattel S (1997). Antisense oligodeoxynucleotides directed against Kv1.5 mRNA specifically inhibit ultrarapid delayed rectifier K^+ current in cultured adult human atrial myocytes. *Circ Res* **80**, 572–579.

Fulop L, Banyasz T, Magyar J, Szentandrassy N, Varro A & Nanasi PP (2004). Reopening of L-type calcium channels in human ventricular myocytes during applied epicardial action potentials. *Acta Physiol Scand* **180**, 39–47.

Gaborit N, Steenman M, Lamirault G, Le Meur N, Le Bouter S, Lande G, Leger J, Charpentier F, Christ T, Dobrev D, Escande D, Nattel S & Demolombe S (2005). Human atrial ion channel and transporter subunit gene-expression remodeling associated with valvular heart disease and atrial fibrillation. *Circulation* **112**, 471–481.

Gao B, Sekido Y, Maximov A, Saad M, Forgacs E, Latif F, Wei MH, Lerman M, Lee JH, Perez-Reyes E, Bezprozvanny I & Minna JD (2000). Functional properties of a new voltage-dependent calcium channel $\alpha_2\delta$ auxiliary subunit gene (CACNA2D2). *J Biol Chem* **275**, 12237–12242.

Goldstein RN & Stambler BS (2005). New antiarrhythmic drugs for prevention of atrial fibrillation. *Prog Cardiovasc Dis* **48**, 193–208.

Gorza L, Schiaffino S & Volpe P (1993). Inositol 1,4,5-trisphosphate receptor in heart: evidence for its concentration in Purkinje myocytes of the conduction system. *J Cell Biol* **121**, 345–353.

Han W, Bao W, Wang Z & Nattel S (2002*a*). Comparison of ion-channel subunit expression in canine cardiac Purkinje fibers and ventricular muscle. *Circ Res* **91**, 790–797.

Han W, Zhang L, Schram G & Nattel S (2002*b*). Properties of potassium currents in Purkinje cells of failing human hearts. *Am J Physiol Heart Circ Physiol* **283**, H2495–H2503.

Kaab S & Nabauer M (2001). Diversity of ion channel expression in health and disease. *Eur Heart J* (Suppl) **3**, K31–K40.

Klugbauer N, Lacinova L, Flockerzi V & Hofmann F (1995). Structure and functional expression of a new member of the tetrodotoxin-sensitive voltage-activated sodium channel family from human neuroendocrine cells. *EMBO J* **14**, 1084–1090.

Kuryshev YA, Gudz TI, Brown AM & Wible BA (2000). KChAP as a chaperone for specific K^+ channels. *Am J Physiol Cell Physiol* **278**, C931–C941.

Lebeche D, Kaprielian R, del Monte F, Tomaselli G, Gwathmey JK, Schwartz A & Hajjar RJ (2004). In vivo cardiac gene transfer of Kv4.3 abrogates the hypertrophic response in rats after aortic stenosis. *Circulation* **110**, 3435–3443.

Li D, Zhang L, Kneller J & Nattel S (2001). Potential ionic mechanism for repolarization differences between canine right and left atrium. *Circ Res* **88**, 1168–1175.

Li X, Zima AV, Sheikh F, Blatter LA & Chen J (2005). Endothelin-1-induced arrhythmogenic Ca^{2+} signaling is abolished in atrial myocytes of inositol-1,4,5-trisphosphate (IP$_3$)-receptor type 2-deficient mice. *Circ Res* **96**, 1274–1281.

Livak KJ & Schmittgen TD (2001). Analysis of relative gene expression data using real-time quantitative PCR and the $2^{-\Delta\Delta C}$T method. *Methods* **25**, 402–408.

Makita N, Bennett PB Jr & George AL Jr (1994). Voltage-gated Na^+ channel β1 subunit mRNA expressed in adult human skeletal muscle, heart, and brain is encoded by a single gene. *J Biol Chem* **269**, 7571–7578.

Malfatto G, Zaza A, Vanoli E & Schwartz PJ (1996). Muscarinic effects on action potential duration and its rate dependence in canine Purkinje fibers. *Pacing Clin Electrophysiol* **19**, 2023–2026.

Mangoni ME, Couette B, Bourinet E, Platzer J, Reimer D, Striessnig J & Nargeot J (2003). Functional role of L-type Cav1.3 Ca^{2+} channels in cardiac pacemaker activity. *Proc Natl Acad Sci U S A* **100**, 5543–5548.

Marionneau C, Couette B, Liu J, Li H, Mangoni ME, Nargeot J, Lei M, Escande D & Demolombe S (2005). Specific pattern of ionic channel gene expression associated with pacemaker activity in the mouse heart. *J Physiol* **562**, 223–234.

Melnyk P, Zhang L, Shrier A & Nattel S (2002). Differential distribution of Kir2.1 and Kir2.3 subunits in canine atrium and ventricle. *Am J Physiol Heart Circ Physiol* **283**, H1123–H1133.

Michels G, Er F, Khan I, Sudkamp M, Herzig S & Hoppe UC (2005). Single-channel properties support a potential contribution of hyperpolarization-activated cyclic nucleotide-gated channels and I$_f$ to cardiac arrythmias. *Circulation* **111**, 399–404.

Nabauer M, Beuckelmann DJ, Uberfuhr P & Steinbeck G (1996). Regional differences in current density and rate-dependent properties of the transient outward current in subepicardial and subendocardial myocytes of human left ventricle. *Circulation* **93**, 168–177.

Nattel S, Matthews C, De Blasio F, Han W, Li D & Yue L (2000). Dose-dependence of 4-aminopyridine plasma concentrations and electrophysiological effects in dogs: potential relevance to ionic mechanisms in vivo. *Circulation* **101**, 1179–1184.

Nattel S, Yue L & Wang Z (1999). Cardiac ultrarapid delayed rectifiers: a novel potassium current family of functional similarity and molecular diversity. *Cell Physiol Biochem* **9**, 217–226.

Plaster NM, Tawil R, Tristani-Firouzi M, Canun S, Bendahhou S, Tsunoda A, Donaldson MR, Iannaccone ST, Brunt E, Barohn R, Clark J, Deymeer F, George AL Jr, Fish FA, Hahn A, Nitu A, Ozdemir C, Serdaroglu P, Subramony SH, Wolfe G, Fu YH & Ptacek LJ (2001). Mutations in Kir2.1 cause the developmental and episodic electrical phenotypes of Andersen's syndrome. *Cell* **105**, 511–519.

Pourrier M, Schram G & Nattel S (2003). Properties, expression and potential roles of cardiac K^+ channel accessory subunits: MinK, MiRPs, KChIP, and KChAP. *J Membr Biol* **194**, 141–152.

Prestle J, Dieterich S, Preuss M, Bieligk U & Hasenfuss G (1999). Heterogeneous transmural gene expression of calcium-handling proteins and natriuretic peptides in the failing human heart. *Cardiovasc Res* **43**, 323–331.

Qu Y, Baroudi G, Yue Y, El-Sherif N & Boutjdir M (2005). Localization and modulation of α1D (Cav1.3), L-type Ca channel by protein kinase A. *Am J Physiol Heart Circ Physiol* **288**, H2123–H2130.

Rhee HM (1981). Accumulation of [^{3}H]-ouabain in functionally different canine cardiac tissues: differential Rb^+ uptake. *Br J Pharmacol* **73**, 81–86.

Rosati B, Dun W, Hirose M, Boyden PA & McKinnon D (2007). Molecular basis of the T- and L-type Ca^{2+} currents in canine Purkinje fibres. *J Physiol* **579**, 465–471.

Rosati B, Grau F & McKinnon D (2006). Regional variation in mRNA transcript abundance within the ventricular wall. *J Mol Cell Cardiol* **40**, 295–302.

Rosati B, Grau F, Rodriguez S, Li H, Nerbonne JM & McKinnon D (2003). Concordant expression of KChIP2 mRNA, protein and transient outward current throughout the canine ventricle. *J Physiol* **548**, 815–822.

Rosati B & McKinnon D (2004). Regulation of ion channel expression. *Circ Res* **94**, 874–883.

Rosati B, Pan Z, Lypen S, Wang HS, Cohen I, Dixon JE & McKinnon D (2001). Regulation of KChIP2 potassium channel β subunit gene expression underlies the gradient of transient outward current in canine and human ventricle. *J Physiol* **533**, 119–125.

Sah R, Ramirez RJ, Oudit GY, Gidrewicz D, Trivieri MG, Zobel C & Backx PH (2003). Regulation of cardiac excitation-contraction coupling by action potential repolarization: role of the transient outward potassium current (I$_{to}$). *J Physiol* **546**, 5–18.

Sakakibara Y, Wasserstrom JA, Furukawa T, Jia H, Arentzen CE, Hartz RS & Singer DH (1992). Characterization of the sodium current in single human atrial myocytes. *Circ Res* **71**, 535–546.

Schram G, Pourrier M, Melnyk P & Nattel S (2002). Differential distribution of cardiac ion channel expression as a basis for regional specialization in electrical function. *Circ Res* **90**, 939–950.

Sridhar A, Lacombe VA, Hamlin RL & Carnes CA (2006). Ultrarapid delayed rectifier current (I_{Kur}) in canine ventricle: Constitutive role in repolarization and reverse use dependence. *Heart Rhythm* **3**, S219–S220.

Thuringer D, Lauribe P & Escande D (1992). A hyperpolarization-activated inward current in human myocardial cells. *J Mol Cell Cardiol* **24**, 451–455.

Ueda K, Nakamura K, Hayashi T, Inagaki N, Takahashi M, Arimura T, Morita H, Higashiuesato Y, Hirano Y, Yasunami M, Takishita S, Yamashina A, Ohe T, Sunamori M, Hiraoka M & Kimura A (2004*a*). Functional characterization of a trafficking-defective HCN4 mutation, D553N, associated with cardiac arrhythmia. *J Biol Chem* **279**, 27194–27198.

Ueda N, Zipes DP & Wu J (2004*b*). Functional and transmural modulation of M cell behavior in canine ventricular wall. *Am J Physiol Heart Circ Physiol* **287**, H2569–H2575.

Varro A, Nanasi PP & Lathrop DA (1993). Potassium currents in isolated human atrial and ventricular cardiocytes. *Acta Physiol Scand* **149**, 133–142.

Verkerk AO, Veldkamp MW, Abbate F, Antoons G, Bouman LN, Ravesloot JH & van Ginneken AC (1999). Two types of action potential configuration in single cardiac Purkinje cells of sheep. *Am J Physiol Heart Circ Physiol* **277**, H1299–H1310.

Xiong W, Tian Y, DiSilvestre D & Tomaselli GF (2005). Transmural heterogeneity of Na^+–Ca^{2+} exchange: evidence for differential expression in normal and failing hearts. *Circ Res* **97**, 207–209.

Yamada KA, Kanter EM, Green KG & Saffitz JE (2004). Transmural distribution of connexins in rodent hearts. *J Cardiovasc Electrophysiol* **15**, 710–705.

Zicha S, Xiao L, Stafford S, Cha TJ, Han W, Varro A & Nattel S (2004). Transmural expression of transient outward potassium current subunits in normal and failing canine and human hearts. *J Physiol* **561**, 735–748.

Acknowledgements

Supplemental material

Online supplemental material for this paper can be accessed at: http://jp.physoc.org/cgi/content/full/jphysiol.2006.126714/DC1 and
http://www.blackwell-synergy.com/doi/suppl/10.1113/jphysiol.2006.126714